Pre- and Postbuckling Finite Element Analysis of Curved Composite and Sandwich Panels

Jean-Pierre Jeusette* and Gottfried Laschet*
Aerospace Laboratory of University of Liège, Liège, Belgium

A three-dimensional degenerated isoparametric multilayer finite element is described in conjunction with an automatic incremental/iterative method to find the complete nonlinear response of arbitrarily laminated composite and sandwich panels under destabilizing loads. The case of thick sandwich panels is investigated by comparing three different models: 1) a high-order, multilayer shell element, 2) a multilayer shell element with null transverse shear moduli in the skins layers, and 3) a superposition of multilayer isoparametric membranes for the skins, and a volume element for the core. All these models allow the accurate representation of the cross-section warping in thick shear deformable sandwich panels and, after some validation tests, the model (3) is found to be the most efficient. In the prebuckling range of the structural response, incremental bifurcation analyses are combined with an arc-length algorithm to control the step size; for the postbuckling path, the increment size is determined automatically by a new recurrence formula. The good behavior of this proposed procedure is illustrated on two structural postbuckling applications, namely, a highly curved cylindrical composite panel and a sandwich panel with flange edges both subjected to in-plane compression.

I. Introduction

ADVANCED composite materials are now widely used in the design of modern aerospace vehicles. Flat and lightly curved panels appear in structures as stabilizers, wings, and mean fuselage, but highly curved panels are present in the rear fuselage zones.[1,2] The aircraft designers often employ thin composite laminated shells and moderately thick sandwich panels or a combination of these two structural components. In flight conditions, these structures are submitted to in-plane forces combined with transverse pressure load that can cause instability phenomena.

Neglecting the possible postbuckling strength of these composite panels constitutes a severe design limitation when weight savings are required. So, the actual tendency is to design composite panels that have a significant postbuckling load-carrying capability.

The understanding of the complex instability phenomena constitutes a new challenge for the designer and stress analyst. In order to find and improve new design procedures, which are actually based only on experimental tests, the development of efficient numerical methods is required to simulate accurately the postbuckling behavior of composite panels.

So, at first, an isoparametric multilayer shell element is generated into a nonlinear finite element program to model either shell composite structures or thick sandwich panels. This element has to provide accurate stresses and strains to predict the failure mechanisms without a prohibitive additional cost. Second, an efficient incremental procedure able to detect and overcome limit points of the equilibrium path is necessary to determine the complete nonlinear response of such panels under destabilizing loads.

In earlier studies,[3,4] only experimental tests were performed. Next, in more recent works, the authors have compared finite element results to experimental ones without really insisting on the finite element model nor on the numerical solution procedures.[1,2,5] In other papers, either the finite element model[6,7] or the solution procedure[8] is described. In the case of sandwich shells, static linear applications are reported in Ref. 9 and postbuckling analyses of thin sandwich shells are presented in Ref. 10. However, the postbuckling finite element analysis of thick sandwich panels with laminated faces and variable core thickness does not appear in the literature.

Thus, the aim of this paper is to describe, at first, the general multilayer element model (Sec. II). After that, in Sec. III, three different formulations are presented to model the thick sandwich shells: 1) a high-order multilayer shell element, 2) a multilayer shell element with null transverse shear molduli in the skin layers, and 3) a superposition of multilayer isoparametric membrances for the skins, and a volume element for the core. Then, the more efficient model is chosen by comparing the numerical results with analytical and experimental ones. After having briefly recalled the proposed automatic solution procedure (Sec. IV), the numerical tool efficiency and accuracy are illustrated on the determination on the nonlinear response of composite and sandwich panels subjected to destabilizing loads (Sec. V).

II. Multilayer Solid and Shell Models

A three-dimensional isoparametric multilayer finite element is developed for the analysis of arbitrarily laminated composite panels. This element is an isoparametric degenerated volume element belonging to the Ahmad shell family[11] extended to a multilayer version in Ref. 12.

The formulation used allows the study of a wide variety of structures: multilayer solid elements and moderately thick and thin laminated shells. In all cases, each node has three translation degrees of freedom. According to the model, each layer can be considered as an orthotropic solid or shell.

In the case of a volume layer, the complete three-dimensional constitutive relations are used.

For the shell model, a 16-nodes element is employed (see Fig. 1). Here, the lines perpendicular to the shell reference surface remain straight but not necessarily normal after deformation; moreover, relaxed constitutive relations are adopted to impose the uncoupling between the shell in-plane and out-of-plane stress components ($\sigma_z = 0$, see Fig. 1 for the local axis systems). However, to avoid mechanisms, the transverse normal stress component is kept different from zero; for that, a normal transverse stiffness is maintained to a value depending on the shell thickness lower than the other diagonal stiffness terms but sufficiently high to avoid a pinching energy overesti-

Received Aug. 15, 1988; revision received May 17, 1989.

*Professor.

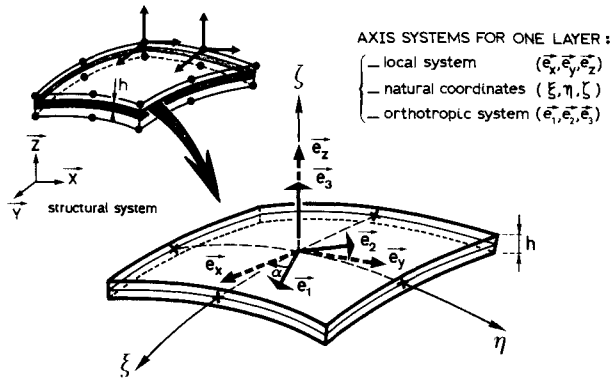

Fig. 1 Three-dimensional degenerated multilayer shell element and the axis systems for a layer.

mation in the case of very thin shells [see factor k in Eqs. (1)].

Moreover, a transverse shear stiffness correction is imposed to take into account a parabolic transverse shear stress distribution through the thickness.

These relaxed orthotropic constitutive relations are summarized in the following notations

$$\sigma_{ii} = C_{ij}^{*}\,\epsilon_{jj} \qquad i,j = 1,2 \tag{1a}$$

$$\sigma_{33} = k\,E_{33}\,\epsilon_{33} \qquad \tau_{12} = G_{12}\,\gamma_{12} \tag{1b}$$

$$\tau_{23} = 5/6\;G_{23}\,\gamma_{23} \qquad \tau_{13} = 5/6\;G_{13}\,\gamma_{13} \tag{1c}$$

where

$$C_{ij}^{*} = C_{ij} - \frac{C_{i3}\,C_{j3}}{C_{33}} \quad i,j = 1,2$$

$k = \beta(h/L)^2$ with $10^{-1} \le \beta \le 10^2$ according to the shell thickness h; L is a characteristic length.

To decrease the computational time, a reduced integration scheme is used over the surface layer. This integration option gives good results (with neither shear nor membrane locking) up to an edge length to thickness ratio (L/h) of 200. Nevertheless, this reduced integration scheme can lead to mechanisms at the element level but they disappear when at least two elements are assembled. The Jacobian matrix is assumed to be constant through the thickness of each layer, therefore, one Gauss point integration in the thickness direction is used to calculate the stiffness matrix of each layer. The element stiffness matrix is evaluated by adding the contributions of each ply.

To take into account the geometrical nonlinearities (large displacement, following forces), a total Lagrange formulation is employed to extend this element. So, all integrations are made on the initial configuration, which constitutes an interesting reference position where the fiber direction in each ply is known.

III. Thick Sandwich Shell Models

For thick sandwich panels ($L/h < 40$), the transverse shear deformation plays an important role. Therefore, this effect has to be considered when determining the response of such panels. Below, three finite element models are described and compared on a simple numerical application. The best one is retained for the postbuckling analysis reported in Sec. V.

A. Models Description

1. Model I

The thick multilayer element (Sec. II) can be used to model the sandwich, but an adequate order has to be chosen for the displacement field through the thickness. Indeed, a first or second degree approximation leads to a too-stiff structural behavior; only a third-degree approximation gives acceptable (still too stiff) results but is, of course, very expensive due to the high degree of freedom number and the numerical integration in each layer of the skins. Besides, as the differences in the mechanical properties are located through the thickness near the interface core/skins, a three-degree interpolation cannot represent exactly the warping of the cross section.

2. Model II

When evaluating the sandwich stiffness matrix with the model I, the contribution of the skins induces an overestimation in the transverse shear stiffness terms due to the great shear moduli difference between the core and the composite skins (for example, 85 MPa with respect to 1600 MPa). An easy way to avoid this problem is to "annul" the transverse shear moduli of the skins, doing a kind of hybrid assumption on setting the transverse shear stresses to zero in the skins. So, this model improves the result's accuracy but remains also expensive due to the numerical integration in each skin layer. Nevertheless, a thick multilayer shell element can be directly adopted to model thick sandwich shells.

3. Model III

For cost and easy connection reasons, a multilayer membrane isoparametric finite element is developed to model the sandwich composite skins, the core being idealized by a monolayer shell/volume finite element as above (note that for honeycomb cores. ν_{13} and ν_{23} are very low, therefore, the shell or volume formulation gives the same results). When the sandwich skins are thin, their bending stiffness contribution can be neglected with respect to the bending stiffness of the whole panel; thus, a membrane element is really adequate and accurate. In this case, the stiffness matrix of the skins contains only an extension contribution evaluated by a classical homogeneization procedure. The extensional stiffness for N layers is given by

$$A_{ij} = \sum_{k=1}^{N} [Q_{ij}]_k\,(z_k - z_{k-1}) \tag{2}$$

where $[Q_{ij}]_k$ is the Hooke matrix of the ply k in a local axis system and z_k the distance from ply k to the neutral axis of the skin. Moreover, modeling the sandwich panel by these 3 elements through the thickness allows the calculation of very accurate interlaminar stresses at the skin-core junction without increasing the degrees of freedom number. Due to the high orthotropy of the honeycomb core and the great moduli difference between the core and the composite skins, a normal surface integration ($3 \times 3 \times 2$) is recommended for the evaluation of the core stiffness matrix in order to avoid numerical parasite flexibility. For isotropic foam cores, a classical reduced integration ($2 \times 2 \times 2$) technique is appropriate.

As the membrane element has no geometrical thickness, the core is modeled up to the half of each skin thickness in order to respect the real geometry, and the core mechanical properties are reduced adequately. Of course, the real properties are used to evaluate the stress state.

Remark: All the three models allow the representation of a variable thickness of the sandwich panel, but model III is the most accurate to follow the geometry in the flange edges zones of the panel.

B. Validation Test

A thick sandwich plate ($L/h = 20$) of which the geometry and boundary conditions are presented on Fig. 2 is subjected to a central transverse load. Therefore, this example is a three-points bending test for which transverse shear deformation is important.

The sandwich is composed by two composite skins and a honeycomb core

1) upper skin lay up: [90 deg; 0 deg]$_3$
2) inner skin lay up: [0 deg; 90 deg]$_3$

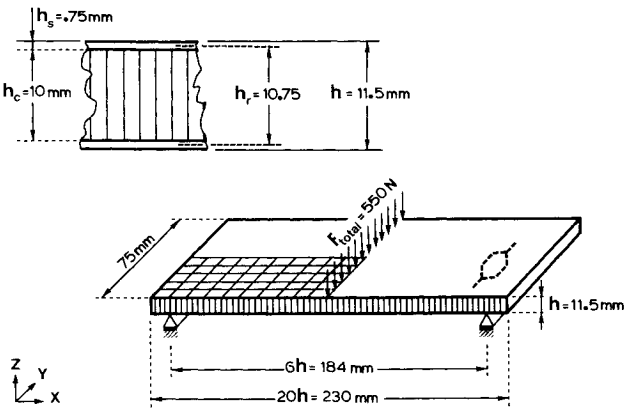

Fig. 2 Sandwich plate: geometry and boundary conditions.

The thickness of each ply is 0.125 mm.

The mechanical properties of the sandwich are the following

1) carbon-epoxy skins

$E_1 = 47$ kN/mm^2 $E_2 = E_3 = 3$ kN/mm^2

$G_{12} = G_{23} = G_{31} = 1.6$ kN/mm^2

$\nu_{12} = \nu_{23} = \nu_{31} = 0.35$

2) honeycomb core

$E_1 = E_2 = 0.005$ kN/mm^2 $E_3 = 0.067$ kN/mm^2

$G_{12} = 0.0030$ kN/mm^2 $G_{13} = 0.021$ kN/mm^2

$G_{23} = 0.071$ kN/mm^2

$\nu_{12} = 0.25$ $\nu_{13} = \nu_{23} = 0.02$

Due to the symmetry, a quarter of the plate is studied and discretized with 10×5 elements for models I and II and with $10 \times 5 \times 3$ elements for model III.

The three models described above have been checked on this application for which the experimental central deflection is 2.30 mm. An analytical calculation based upon a flat rectangular beam theory[13] gives a central deflection value of 2.33 mm.

The central deflection of each skin and the CPU time of each analysis reported to model III CPU time are presented in Table 1. All these cases have been run with a second degree displacement field leading to a 2079 degree of freedom discretization. Only the study B in Table 1 corresponds to a third-degree interpolation and 2872 degree of freedom. In the multilayer models I and II, a ply means either a skin layer or the core considered as a ply.

Model I shows bad results for a second (case A) or third (case B) degree displacement field.

The results with model II (cases D, E, and F) are quite good but with a relatively high computational cost. However, the case C gives wrong results due to the reduced integration used for the core; moreover, the use of a $2 \times 3 \times 1$ scheme does not improve these results but a $3 \times 2 \times 1$ scheme gives the same good results as case D; indeed, an exact integration in the X direction is required to compensate the lower value of the transverse shear modulus in this direction. In conclusion, the choice of the number of integration points in the core is related to the honeycomb material properties in order to avoid numerical parasite flexibility.

Finally, model III (cases G and H) provides good results and the lowest CPU time.

C. Model Choice

According to this validation test, model III is found to be the most efficient, and it will be used for the postbuckling sandwich application.

IV. Automatic Incremental/Iterative Method

The automatic incremental/iterative scheme used is briefly recalled. More detailed information can be found in Ref. 14.

Table 1 Central deflection results for a sandwich plate subjected to a three-points bending test

	Central deflection (mm)		CPU
	Above	Below	CPU model III
A Model I $2 \times 2 \times 2$ Gauss points/ply	0.6691	0.6585	1.74
B Model I 3rd degree $2 \times 2 \times 2$ Gauss points/ply	1.7237	1.6882	2.32
C Model II $2 \times 2 \times 1$ Gauss points/ply ou $2 \times 3 \times 1$ (idem)	3.3487	2.2050	1.22
D Model II $3 \times 3 \times 1$ Gauss points/ply ou $3 \times 2 \times 1$ (idem)	2.2718	2.2417	1.86
E Model II $2 \times 2 \times 2$ Gauss points/ply	2.2141	2.1389	1.74
F Model II $3 \times 3 \times 2$ Gauss points/ply	2.1760	2.1485	2.90
G Model III 2×2 G. p. in the skins $3 \times 3 \times 2$ G. p. in the core	2.3013	2.1480	1.10
H Model III 2×2 G. p. in the skins $2 \times 2 \times 2$ G. p. in the core	2.3504	2.1154	1
I Experimental result	2.30		—
J Analytical result	2.33		—

A. Prebuckling Analysis

First, an initial bifurcation analysis is performed to introduce eventually a geometrical imperfection and to choose the first step load level from the estimated critical load. The initial stability problem leads to an eigenvalue problem including the initial stiffness matrix and the stability matrix based upon a linearization of the fundamental path. The contributions of the geometrical, initial displacement and following forces stiffness matrices can be included in the stability matrix evaluation.

Next, an incremental bifurcation analysis is applied on some deformed configurations of the prebuckling equilibrium path to give an optimal selection of the step size for an incremental/iterative solution method in the load-displacement space and to detect the proximity of eventual bifurcation points on the nonlinear equilibrium path. The load-displacement space algorithm is described in Ref. 14.

B. Postbuckling Analysis

As for the prebuckling range, the postbuckling part of the nonlinear response has to be traced by using only a few steps to describe the less interesting unstable zone and to reach, with accuracy, a next critical point giving a plausible inferior limit to the real critical load.

Therefore, the step sizes are controlled by recurrence formula described in Ref. 14.

V. Numerical Buckling and Postbuckling Applications

The described finite elements and the automatic solution procedure are implemented into the Système d'Analyse de Milieux Continus jon Eléments Finis program. To illustrate the method efficiency, some instability problems of composite and sandwich panels are presented. First, the nonlinear response of a highly curved cylindrical shell subjected to in-plane compression is analyzed. Then, a typical sandwich panel with flange edges under axial compression is studied.

A. Highly Curved Multilayer Composite Cylindrical Shell under Axial Compression

Snell and Morley[1] have determined by numerical analysis and experimental tests the pre- and postbuckling behavior of highly curved composite panels with different lay ups under axial compression. For this kind of shells, the imperfection sensitivity is important so that usually the experimental buckling load is lower than the theoretical one. Furthermore, these panels have a postbuckling behavior that presents a severe snap back and a steep negative slope. This application constitutes a severe test of the proposed step size method.

The multilayer cylindrical shell (see Fig. 3a) is simply supported along its straight edges and clamped at its curved edges. Its geometrical properties are shown in Fig. 3a. The panel is built up by a symmetric lay up (45 deg; −45 deg; −45 deg; 45 deg; $0_4)_S$ where the ply thickness is equal to 0.125 mm. The material characteristics of the carbon-epoxy XAS-914C layers are

$$E_1 = 130 \text{ kN/mm}^2; \qquad E_2 = E_3 = 10 \text{ kN/mm}^2$$

$$G_{12} = 6 \text{ kN/mm}^2; \qquad \nu_{12} = 0.3$$

The axial compressive load is applied by a uniform displacement increase at one curved edge.

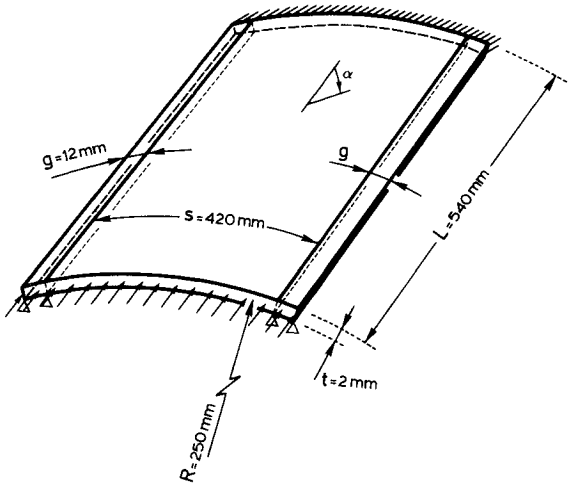

Fig. 3a Highly curved multilayer cylindrical shell under axial compression: geometry.

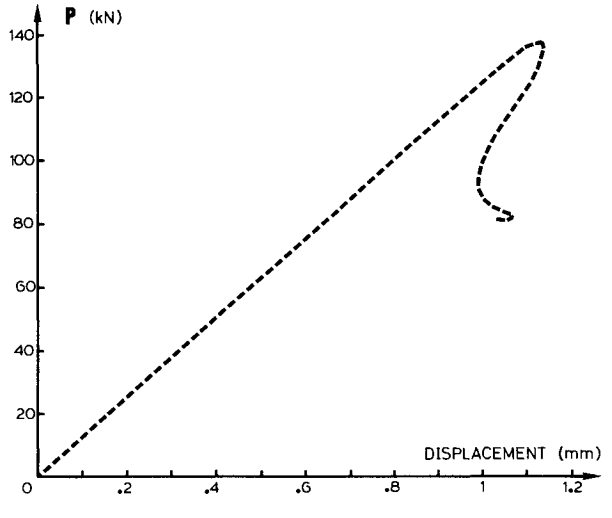

Fig. 3b Load-displacement curve.

Table 2 Comparison of buckling loads

Authors	Analysis Method	Mesh	Buckling load (KN)	Comparison to exp. (%)
Snell & Morley [1]	Experiment		134.	—
	STAGCS			
	a) linear	20 × 20	149.2	11.34%
	b) nonlinear	20 × 20	151.5	13.06%
Jun & Hong [6]	linear	8 × 10	143.2	6.87%
Present analysis	SAMCEF			
	a) linear	8 × 10	143.9	7.4 %
	a) nonlinear		137.8	2.83%
	linear	12 × 18	140.24	4.66%

Snell and Morley use the STAGSC-1 finite element code to verify their experimental results and to modelize the cylindrical panel with a fine 20 × 20 mesh of flat Clough plate elements (36 degrees of freedom).

1. *Bucking Results*

The linear and nonlinear bifurcation results of Snell and Morley are summarized in Table 2.

In a first step, a coarse 8 × 10 mesh is adopted. In this model, second degree isoparametric multilayer shell elements with 2 × 2 × 1 integration points per layer are used leading to a model with 1454 degrees of freedom. Jun and Hong[6] used the same coarse mesh with an equivalent multilayer shell element.

As shown in Table 2, the present analysis gives more accurate buckling loads with a coarser mesh than the Snell and Morley one. The correct geometry representation and the reduced integration technique explain the better behavior of this element. Moreover, it is normal that the nonlinear analysis provides a lower buckling load and that our linear bifurcation analysis gives approximately the same results as the Jun analyses.

Finally, to improve our results, a finer mesh with 12 × 18 elements is realized, which provides a buckling load reduction of 2.74%. The first buckling mode obtained with the fine mesh presents 5 bulges as illustrated in Fig. 4. The corresponding buckling load equals to 140.245 kN. The second buckling load is 142.24 kN: that indicates the presence of clustered bifurcation points instead of a simple bifurcation phenomenon.

2. *Nonlinear Response*

At first, an initial end displacement of 0.5 mm is applied corresponding to a compression reference load of 63.086 kN ($\lambda = 1.$). At this prebuckling state, the cylindrical shell has a tendency to barrel outwards. This barreling effect, illustrated in Fig. 5 on the deformed shape, is also observed in the test experience and is due to the clamped edges. Note that the small out-of-plane displacements transform the bifurcation

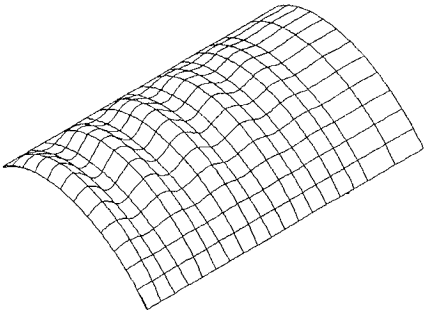

Fig. 4 Composite cylindrical shell: first buckling mode of linear stability analysis (fine mesh 18*12 elements).

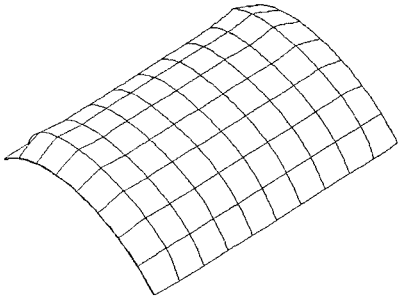

Fig. 5 Composite cylindrical shell: prebuckling deformed shape at P = 63.086 kN (coarse mesh 10*8 elements).

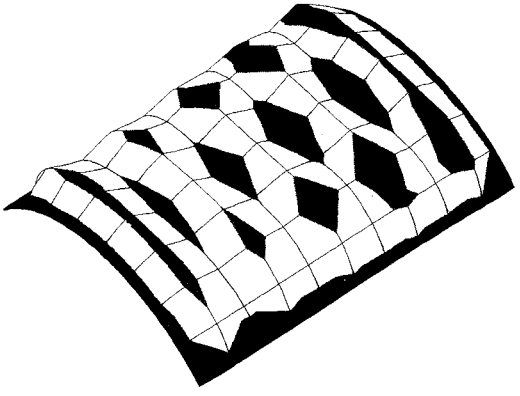

Fig. 6 Composite cylindrical shell: initial postbuckling mode at P = 137.47 kN (non-linear analysis).

point into a limit point, which can be passed using the proposed automatic incremental/iterative method described in section IV. The quasilinear prebuckling response permits definition of great load-displacement increments, which are applied without additional stability analysis.

At the third increment, the limit point is passed ($\lambda = 2.179$), and the panel buckles in a 5-bulges mode (see Fig. 6) that is modulated by a circonferential wave with two peaks. At this buckling load, the shell undergoes an important energy drop caused by the stiffness change from a predominant membrane behavior to a combined membrane and bending action. In the experimental test, the shell drops dynamically to a 43% lower load (76.4 kN).[1]

The postbuckling path has been chosen parallel to the first buckling mode, but it is possible that the real postbuckling trajectory be a combination of the two first modes.

To describe the unstable path with a severe snap back and a deep negative slope, an important reduction of the load-displacement factor, η, is necessary ($\Delta\eta = 5.E^{-02}$) to initialize the automatic iterative procedure. Then, several unloading increments (18) have been applied. The corresponding load-displacement response is plotted in Fig. 3b. During the decrease the postbuckled deformation shapes become, as shown on Fig. 7 for a load level $\lambda = 1.72$, simpler with fewer and deeper bulges (two peaks and a central hole) than the initial buckling mode.

At the 22nd increment, a reduction of the end shortening is observed, and the algorithm converges slowly (6 iterations). At the next step, the number of negative pivots increases (=2) and complex roots of the arc-length constraint appear. After further step sizes reductions, an oscillation of the negative pivots number is observed during the iterative process; that indicates clearly the presence of clustered bifurcations points.

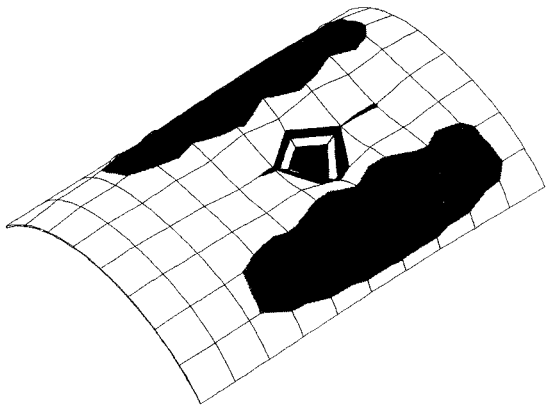

Fig. 7 Composite cylindrical shell: unstable postbuckled shape at P = 108.5 kN .

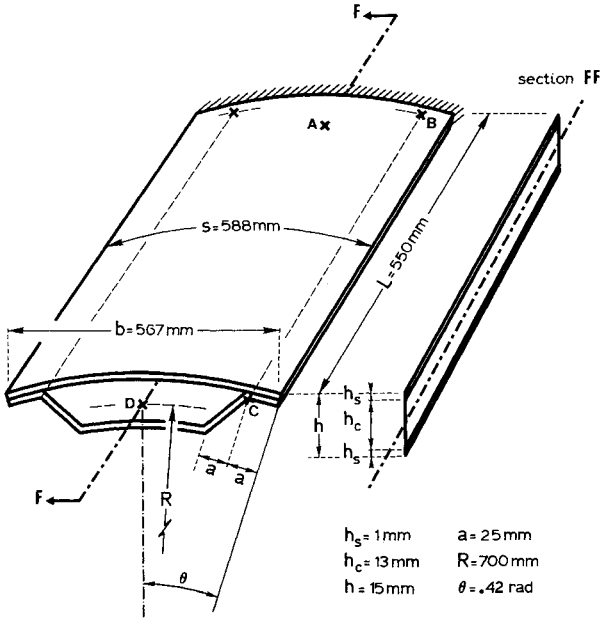

Fig. 8 Sandwich cylindrical panel with flange edges under axial compression: geometry.

Moreover, the branch chosen by the program (not entirely shown in Fig. 3b) is wrong, and that leads to a "come-back" response! Therefore, further investigations of clustered bifurcations points are necessary to go on with the panel response description.

B. Sandwich Cylindrical Panel with Flange Edges Subjected to In-plane Compression

A sandwich panel typically used in aircraft structures is studied now. The geometrical properties of this thick cylindrical shell ($L/h = 40$) are described in Fig. 8. This moderately curved panel is clamped on both curved edges and simply supported on the straight edges. Near the supports, the panel section is reduced to easily attach the panel to the next one and/or to the stiffeners.

The sandwich is composed of two composite tape skins and a honeycomb core

1) upper skin lay up: [90 deg; 0 deg; 90 deg; 0 deg]
2) inner skin lay up: [0 deg; 90 deg; 0 deg; 90 deg]

The thickness of each tape ply is 0.25 mm.

The mechanical properties of the sandwich are the following.

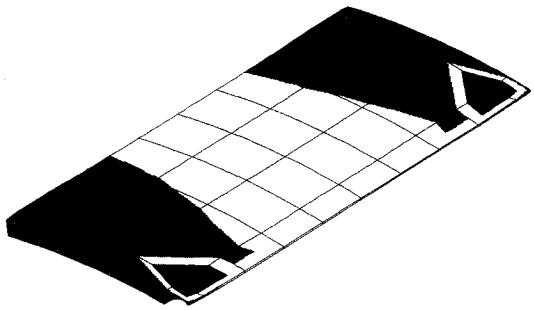

Fig. 9 Sandwich panel: prebuckling deformed shape.

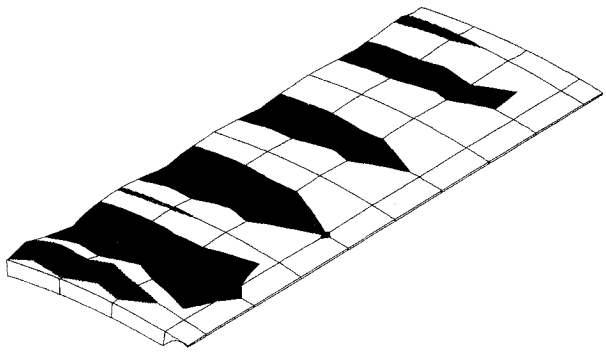

Fig. 10 Sandwich panel: first critical mode at P = 127.83 kN.

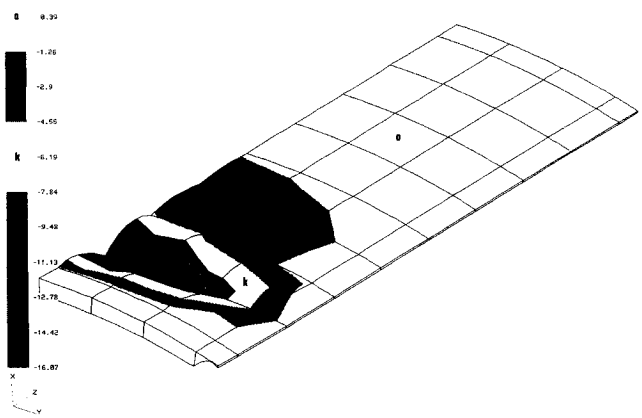

Fig. 11 Sandwich panel: postbuckling mode at P = 115.29 kN .

1) skins: carbon-epoxy Fabric 6803/5208 NARMCO tape:

$E_1 = 67.57$ kN/mm^2; $E_2 = 64.81$ kN/mm^2; $E_3 = 11.72$ kN/mm^2

$$G_{12} = G_{23} = G_{31} = 5.03 \text{ kN/mm}^2$$

$$\nu_{12} = 0.05; \quad \nu_{23} = \nu_{31} = 0.3$$

2) honeycomb core

$$E_1 = E_2 = 1.E^{-04} \text{ kN/mm}^2; \qquad E_3 = 0.141 \text{ kN/mm}^2$$

$$G_{12} = 1.E^{-05} \text{ kN/mm}^2; \qquad G_{13} = 0.0246 \text{ kN/mm}^2$$

$$G_{23} = 0.0492 \text{ kN/mm}^2$$

$$\nu_{12} = 0.25; \qquad \nu_{13} = \nu_{23} = 0.02$$

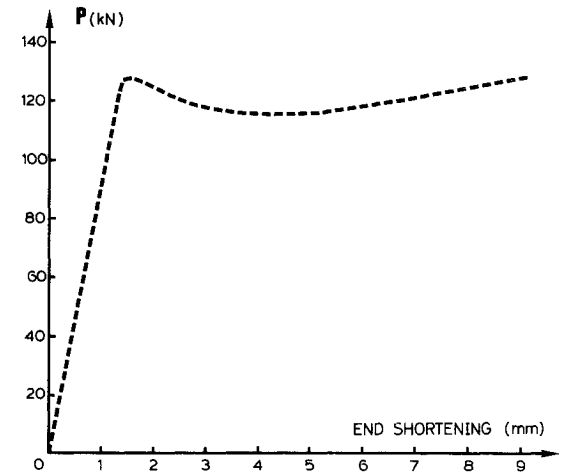

Fig. 12a Sandwich cylindrical panel with flange edges under axial compression: load-end shortening curve.

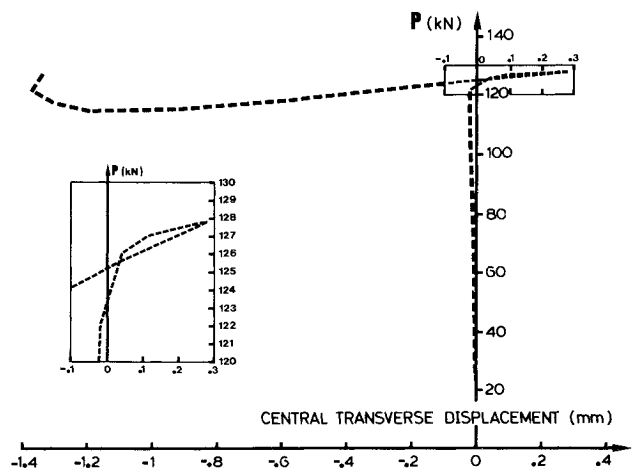

Fig. 12b Load-central transverse displacement curve.

1. Model

Due to the symmetry, a half of the shell is studied, and appropriate symmetry boundary conditions are imposed.

The sandwich core is modeled by monolayer isoparametric solid elements with $3 \times 3 \times 2$ Gauss integration points. The skins are modeled by multilayer isoparametric membrane elements with a reduced integration (2×2) scheme. So, the mesh has $8 \times 10 \times 3$ elements corresponding to a 663 degrees of freedom discretization. Model III is only used in this analysis.

The flange edges where the honeycomb core vanishes are considered to be rigid, simulating the stiffener's effect. The boundary conditions are imposed as follows (see Fig. 8): the lines *AB-CD* are clamped, and the line *BC* is simply supported. The axial compressive load is applied by a uniform displacement increase at one curved edge.

2. Nonlinear Response

An initial end shortening displacement of 1 mm is applied at one curved edge corresponding to a compression load of 96.49 kN. Due to the flange edges, the eccentricity of the load causes an initial imperfection (inwards bending near the points *B* and *C* in Fig. 8). An outwards barreling appears near both clamped edges. This transverse displacement field transforms the bifurcation instability into a limit point behavior. The prebuckling deformed shape is shown in Fig. 9 for the half panel.

The equilibrium path is linear up to the limit point that occurs for a compression load of 127.83 kN, nearly identical to the buckling load obtained by an initial bifurcation analysis. At this critical load, the panel buckles in a 5-bulges mode modulated by a half wave in the circonferential direction (see Fig. 10).

After having passed this first limit point, the panel response describes a relatively short unstable path up to a second limit point at which the compression load equals to 115.29 kN. As shown in Fig. 11, the postbuckling deformed shape corresponding to this stable equilibrium point becomes simpler and deeper and is located near the loaded edge.

Finally, the load/end shortening and the load/central transverse displacement responses are presented respectively in Fig. 12a and Fig. 12b. These curves illustrate clearly that the panel exhibits postbuckling strength.

VI. Concluding Remarks

A multilayer shell element and an automatic incremental/iterative method are used as useful tools to study the pre- and postbuckling behavior of arbitrarily laminated composite and sandwich panels.

The applications illustrate that the developed shell element allows the modelization of a wide variety of composite panels. However, due to the numerical integration of the stiffness matrix, its generation time is important for a large number of plies. In order to reduce the computational cost, a new homogeneization technique compared with an analytical preintegration through the thickness (see Ref. 15) is under investigation.

Its use in conjunction with multilayer membranes is really adequate for thick sandwich modelizations with variable core thickness.

The automatic incremental/iterative scheme works very well for snap-through collapses (see Ref. 14). Nevertheless, in the case of the first application, the severe snap-back is difficult to trace automatically. The future developments in this area will consist of developing criteria that detect a corrector phase divergence as soon as possible and will determine what action needs to be taken in case of divergence or complex roots detection (for example, doing a restart of the increment with a step size reduction).

Finally, as illustrated in the first application, the presence of clustered bifurcations points is a source of difficult numerical problems. To overcome these difficulties, a future development will consist of determining the combination of the clustered bifurcations modes, which minimizes the strain energy for a given perturbation amplitude, as suggested in Ref. 16.

Acknowledgments

The authors wish to express their gratitude to their colleagues T. Duesberg and A. Remouchamps for discussions about the sandwich modelization and are also grateful to the Belgian Research Institute IRSIA for supporting this work.

References

[1]Snell, M. and Morley, N., "The Compression Buckling Behavior of Highly Curved Panels of Carbon Fibre Reinforced Plastic," *Proceedings of Fifth International Conference of Composite Materials,* Harrigan, Strife, and Dhingra, San Diego, 1985, pp. 1327–1353.

[2]Wiggenraad, J., "The Postbuckling Behavior of Blade-Stiffened Carbon-Epoxy Panels Loaded in Compression," *Proceedings of Fifth International Conference of Composite Materials,* Harrigan, Strife, and Dhingra, San Diego, 1985, pp. 1377–1392.

[3]Romeo, G., "Experimental Investigation on Advanced Composite-Stiffened Structures under Uniaxial Compression and Bending," *AIAA Journal,* Vol. 24, Nov. 1986, pp. 1823–1830.

[4]Khot, N. and Bauld, N., "Further Comparisons of the Numerical and Experimental Buckling Behavior of Composite Panels," *Computers & Structures,* Vol. 17, 1983, pp. 61–68.

[5]Starnes, J., Knight, N., and Rouse, M., "Postbuckling Behavior of Selected Flat Stiffened Graphite-Epoxy Panels Loaded in Compression," *AIAA Journal,* Vol. 23, Aug. 1985, pp. 1236–1246.

[6]Jun, S. M. and Hong, C. S., "Buckling Behavior of Laminated Composite Cylindrical Panels under Axial Compression," *Computers & Structures,* Vol. 29, 1988, pp. 479–490.

[7]Saigal, S., Kapania, R., and Yang, Y., "Geometrically Non-Linear Finite Element Analysis of Imperfect Laminated Shells," *Journal of Composite Materials,* Vol. 20, 1986, pp. 197–214.

[8]Petiau, C. and Cornuault, C., "Algorithmes Efficaces pour le Calcul des Equilibres en Post-Flambement," *Proceedings of 3ième Colloque sur les Tendances Actuelles en Calcul des Structures,* Grellier and Campel, Bastia, 1985, pp. 109–127.

[9]Holt, P. J. and Webber, J. P., "Finite Elements for Honeycomb Sandwich Plates and Shells, Part 1: Formulation of Stiffness and Consistent Load Matrices," *Aeronautical Journal,* March/April 1980, pp. 113–123.

[10]Schmit, L. A. and Monforton, G. R., "Finite Deflection Discrete Element Analysis of Sandwich Plates and Cylindrical Shells with Laminated Faces," *AIAA Journal,* Vol. 8, Aug. 1970, pp. 1454–1461.

[11]Ahmad, S., Irons, B. M., and Zienkiewicz, O. C., "Analysis of Thick and Thin Shell Structures by Curved Finite Elements," *International Journal of Numerical Methods in Engineering,* Vol. 2, 1970, pp. 419–451.

[12]Chao, W. and Reddy, J., "Analysis of Laminated Composite Shells Using a Degenerated Three-Dimensional Element," *International Journal of Num. Meth. Engineering,* Vol. 20, 1984, pp. 1991–2007.

[13]Doc. HEXCEL TSB124, "The Basics on Bonded Sandwich Construction," 1987.

[14]Jeusette, J.-P., Laschet, G., and Idelsohn, S., "An Effective Automatic Incremental/Iterative Method for Static Nonlinear Structural Analysis," *Computers & Structures,* Vol. 32, 1989, pp. 125–135.

[15]Stanley, G. M., Park, K. C., and Hughes, T. J. R., "Continuum-Based Resultant Shell Elements," Finite Element Methods for Plate and Shell Structures, Vol. 1, Element Technology, Swansea, 1986, pp. 1–45.

[16]Carnoy, E. and Panosyan, G., "Méthodes Numériques pour l'Analyse du Flambage Elastoplastique de Structures Complexes," *Proceedings of 3ième Colloque sur les Tendances Actuelles en Calcul des Structures,* Bastia, 1985, pp. 145–162.